9.5 DPATC – Dual-Pol based Attenuation Correction

Concept

Due to precipitation, the radar radiation is attenuated. An algorithm to correct reflectivity for attenuation, based on the reflectivity data only, is described in chapter 9.4. That ZATC algorithm has the disadvantage that the attenuation correction might be too weak or might become instable, depending on the accuracy of the Z-R relation used therein. In case of polarimetric radar systems, the differential reflectivity (ZDR) also suffers from attenuation effects, since the horizontally polarized radiation usually is attenuated stronger than the vertical polarized attenuation, resulting in negatively biased ZDR data.

For a fully polarimetric radar system, the differential phase shift provides more stable measurement of the attenuation. Furthermore, ZDR bias from differential attenuation can also be corrected for. The dual-pol based attenuation correction algorithm (DPATC) performs the corresponding correction of dBZ and, if available, ZDR data.

The algorithm can be applied on any scan type (azimuth scan, volume scan, or elevation scan) which samples reflectivity data and differential phase data (PhiDP). The scan may also contain ZDR data, which then also are corrected. Note that the PhiDP data are usually already filtered according to the algorithm described in chapter 9.6.

Product Definition

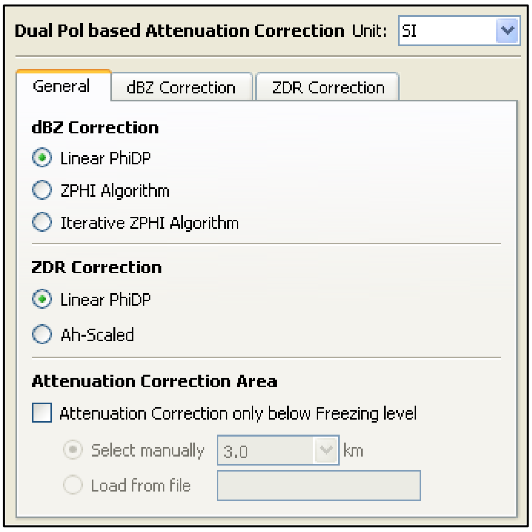
Dual Pol based Attenuation Correction Unit: SI

dBZ Correction
● Linear PhiDP
○ ZPHI Algorithm
○ Iterative ZPHI Algorithm

ZDR Correction
● Linear PhiDP
○ Ah-Scaled

Attenuation Correction Area
☐ Attenuation Correction only below Freezing level
● Select manually 3.0 km
○ Load from file

Fig. 123: DPATC–General

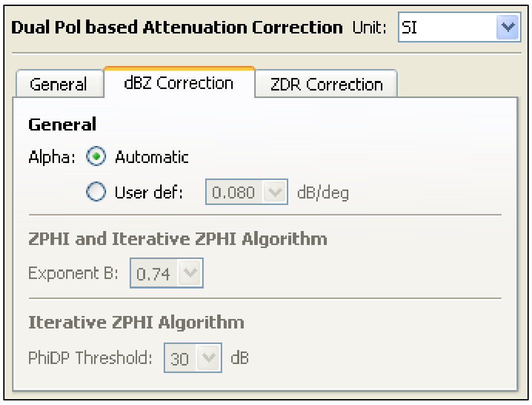
Dual Pol based Attenuation Correction Unit: SI

General
Alpha: ● Automatic
○ User def: 0.080 dB/deg

ZPHI and Iterative ZPHI Algorithm
Exponent B: 0.74

Iterative ZPHI Algorithm
PhiDP Threshold: 30 dB

Fig. 124: DPATC–dBZ Correction

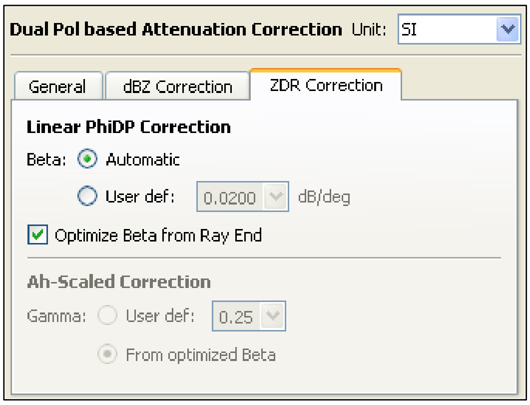
Dual Pol based Attenuation Correction Unit: SI

Linear PhiDP Correction
Beta: ● Automatic
○ User def: 0.0200 dB/deg
☑ Optimize Beta from Ray End

Ah-Scaled Correction
Gamma: ○ User def: 0.25
● From optimized Beta

Fig. 125: DPATC–ZDR Correction

A – General parameters

dBZ Correction (⇒ steps 1, 2 and 3)

Linear PhiDP	dBZ attenuation correction linear in PhiDP
ZPHI Algorithm	dBZ attenuation correction using the ZPHI-Algorithm (option)
Iterative ZPHI Algorithm	dBZ attenuation correction using an iterative ZPHI-Algorithm (option)

ZDR Correction (⇒ steps 4 and 5)

Linear PhiDP	ZDR attenuation correction is linear in PhiDP
Ah-scaled	ZDR attenuation correction proportional to the dBZ correction

Attenuation Correction Area (⇒ step 7)

Atten Corr only below freezing level	Perform attenuation correction only for rain (below freezing level) Height of freezing level: "Select manually" ⇒ by entering a value. "Load from file" ⇒ located in `sensordata`/.

B – dBZ Correction parameters

General (⇒ step 1)

Alpha automatic	Uses a fixed α for the attenuation relation (automatic for the radar wavelength)
Alpha user-def	Uses the given user-defined α for the attenuation relation

ZPHI and Iterative ZPHI Algorithm parameters (⇒ steps 2 and 3)

Exponent B	The exponent b of the ZPHI attenuation equation
PhiDP threshold	The threshold of total path PhiDP, below which the iteration is not used

C – ZDR Correction parameters

Linear PhiDP Correction (⇒ step 4)

Beta automatic	Uses a fixed β for the ZDR attenuation relation (automatic for the radar wavelength)
Beta user-def	Uses the given user-defined β for the ZDR attenuation relation
Optimize Beta	Uses an optimization method for β based on far-range data (⇒ step 6)

Ah-scaled parameters (⇒ step 5)

Gamma user-def	Uses the given user-defined γ for the scaling relation
Gamma from optimized Beta	Calculates the scaling parameter γ from a ZDR attenuation relation parameter b which was optimized from far range data (⇒ step 6)

Algorithm

The correction of attenuation and differential attenuation using dual-polarization data follows the procedures described in the Gematronik Dual-Polarization Handbook (Gematronik, 2007). In particular, the following correction methods can be selected:

Correction of reflectivity:

- Linear PhiDP method (Gematronik, 2007; chapter 4.1) (⇒ step 1)
- ZPHI Algorithm (optional) (⇒ step 2)
- Iterative ZPHI Algorithm (optional) (⇒ step 3)

Correction of differential reflectivity:

- Linear PhiDP method (Gematronik, 2007; chapter 5.1) (⇒ step 4)
- Ah-scaled method (Gematronik, 2007; chapter 5.2) (⇒ step 5)

The correction methods are performed on ray basis, i.e. each ray of data is processed independently. Thus the correction can be applied to any scan: AZI, VOL, ELE.

All methods are based on filtered differential phase data (PhiDP). For such filtered PhiDP, data are only given in areas of sufficient PhiDP accuracy. Furthermore, the PhiDP system offset has been taken into account, i.e. PhiDP values start with 0 deg for small ranges. For details of the PhiDP filtering, please refer to chapter 9.6.

1) dBZ-Correction using the linear PhiDP method

For this correction, the total path attenuation of dBZ, i.e. the amount of correction along radar range r, is proportional to PhiDP:

$$dBZ_{Corr}(r) = dBZ(r) + \alpha \cdot PhiDP(r) \tag{1}$$

The proportionality factor α can be selected according to the “General” parameters of the “dBZ Correction” part:

- Automatic: α is selected automatically according to the radar frequency:
  - S-Band: α = 0.018 dB/deg
  - C-Band: α = 0.08 dB/deg
  - X-Band: α = 0.25 dB/deg
- User-def: The selected (user-defined) value of α is used.

2) dBZ-Correction using the ZPHI Algorithm (optional)

ZPHI is an attenuation correction algorithm which uses a scheme described by Hitschfeld and Bordan (1954) (cf. chapter 9.4 of the Products and Algorithms Manual), and takes the total attenuation, derived from the total PhiDP, as a constraint.

According to Hitschfeld and Bordan (1954), the attenuation coefficient A (in dB/km) can be calculated from the true reflectivity factor Z (in mm^6/m³) by

$$A(r) = a\, Z^b(r) \tag{2a}$$

The path attenuation P (in dB) is then the integrated attenuation coefficient, i.e.

$$P(r) = \int_{r_0}^{r} A(s)ds = 10\log_{10}\left(\exp\left(0.46 \int_{r_0}^{r} A(s)ds \right)\right) \tag{2b}$$

The true reflectivity Z results from the measured reflectivity Z_{meas} and the path attenuation:

$$Z(r) = Z_{meas}(r)\exp\left(0.46\int_{r_0}^{r} A(s)ds\right) = Z_{meas}(r)\exp\left(0.46\, a\int_{r_0}^{r} Z^b(s)ds\right) \tag{2c}$$

This can be integrated to obtain an equation combining the total path attenuation $P_{tot} := \int_{r_0}^{r_1} A(s)ds$ with the distribution of the measured reflectivity Z_{meas} along range. Since the factor a in (2a) has some uncertainty and the radar may not always calibrated perfectly, the such calculated total path attenuation tends to be somewhat unstable.

On the other hand, the total path attenuation is related to the total differential phase shift, as e.g. in Ryzhkov and Zrnić (1995), their eq. (5):

$$P_{tot} = \alpha\,(\Phi_{dp}(r_0) - \Phi_{dp}(r_1)) \tag{2d}$$

Equation (2d) also results from integration of equation (1) in the above described linear PhiDP method.

This means that the total phase shift can be used as a constraint to adjust either a or Z_{meas} (which mathematically means the same) in equation (2c). By that, adjusted attenuation coefficients A' are obtained, which are then used in the central part of equation (2c) to obtain an adjusted distribution of corrected reflectivity Z(r), fitting to the total path attenuation obtained from the total differential phase shift.

An early algorithm called ZPHI (Testud et al., 2000) was based on measured PhiDP data. However, measured data may be biased e.g. by non-meteorological targets or measurements with too low intensity. Furthermore, the measured PhiDP has limited accuracy, i.e. the measured total differential phase shift may significantly differ from theory and can even become negative. These shortcomings are overcome here by using different input data, namely filtered PhiDP data, in the ZPHI algorithm. The total differential phase shift therefore is obtained from sophisticated filtering and smoothing algorithms that are applied to the measured PhiDP data.

3) dBZ-Correction using the Iterative ZPHI Algorithm (optional)

Bringi et al. (2001) improved the attenuation correction using the ZPHI algorithm. According to them, the parameter α should not be taken as fixed. Instead, using any value of α, a PhiDP(r) profile can be re-constructed, and an error function can be defined as the difference between the filtered and the re-constructed PhiDP(r) profile:

$$Error = \sum_{j=1}^{N} \left| \Phi_{dp}^{filt}(r_j) - \Phi_{dp}^{c}(r_j;\alpha) \right| \tag{3}$$

In an iterative approach, an optimum value of α can be found where the error function becomes minimal.

There are two caveats for this iteration:

- The iteration tends to become instable if the total PhiDP is small. Thus it is omitted (and the normal ZPHI algorithm is used with the initial α), when the total PhiDP is smaller than the 'PhiDP Threshold' from the PPDF parameters.
- It may happen that the iteration converges for values of α which are not meaningful. In that case, an optimized α is taken which is very close to the initial α.

4) ZDR-Correction using the Linear PhiDP method

Due to oblate particles like medium-size or big raindrops, ZDR experiences a negative bias because the horizontal radiation is stronger attenuated than the vertical radiation. PhiDP can also be used to correct for that kind of attenuation.

For this the linear PhiDP, the total differential attenuation, i.e. the amount of ZDR correction along radar range r, is proportional to PhiDP:

$$ZDR_{Corr}(r) = ZDR(r) + \beta \cdot PhiDP(r) \tag{4}$$

The proportionality factor β can be selected according to the “Linear PhiDP correction” parameters of the “ZDR Correction” part:

- Automatic: β is selected automatically according to the radar frequency:
  - S-Band: β = 0.0025 dB/deg
  - C-Band: β = 0.02 dB/deg
  - X-Band: β = 0.035 dB/deg
- User-def: The selected (user-defined) value of β is used.

Observations have shown that the proportionality factor β is not constant. Thus the above scheme might cause an over- or under-correction of ZDR. For that reason β can be optimized if “Optimize beta from ray end” is selected. See step 4 for the detailed description.

5) ZDR-Correction using the Ah-scaled method

The assumption that both the dBZ and ZDR attenuation are proportional to PhiDP means that there is also a proportionality between the amount of dBZ correction and the amount of ZDR correction. Using eqs. (1) and (2), the proportionality factor between these two amounts is just $\gamma = \beta / \alpha$; i.e.

$$ZDR_{Corr}(r) - ZDR(r) = \gamma \cdot \left[dBZ_{Corr}(r) - dBZ(r)\right] \tag{5}$$

Such a method for the ZDR correction is called the “Ah-scaled” method (where “Ah” means the specific attenuation of horizontal reflectivity).

If both dBZ and ZDR are corrected using the Linear PhiDP method, this means also that the ZDR correction is “scaled” to the dBZ correction. However, if the dBZ correction is performed using the ZPHI or the iterative ZPHI algorithm, an “Ah-scaled” correction of ZDR according to eq. (5) means that the ZDR correction is not linear with PhiDP, but proportional to the amount of dBZ correction.

The proportionality factor γ is given from the PPDF parameters:

- User-def: The selected (user-defined) value of γ is used.
- From optimized beta: An optimized proportionality factor β_{Opt} is derived (see step 6), and γ is then calculated from this β_{Opt} and the previously given α (see step 1), using $\gamma\ \beta_{Opt} / \alpha$.

6) Optimization of β and γ

According to a method proposed by Bringi et al. (2001) and as described in Gematronik (2007; see eq. (5.3) and figs. 5.1 to 5.3), theoretical values of ZDR can be estimated based on dBZ values: At the (ray’s) end of a precipitation system, i.e. in a rather stratiform area, the ZDR values should be close to zero dB for very week rain, and can be related to the (already corrected) dBZ values for light rain according to Figs. 5.1 to 5.3 of Gematronik (2007). This allows a calculation of theoretical estimates of the proportionality factors β and γ using eq. (5.3) of Gematronik (2007).

“Optimization” here means that a quality parameter (or: weight factor) w between 0.0 and 1.0 is determined together with the theoretical estimate β_{Est} according to eq. (5.3) of the DP-Handbook. The optimized proportionality factors β_{Opt} and γ_{Opt} for each ray are then calculated as a weighted average of the initial values and the theoretical estimates:

$$\beta_{Opt} = w \cdot \beta_{Est} + (1 - w) \cdot \beta \tag{4a}$$

$$\gamma_{Opt} = \beta_{Opt} / \alpha \tag{4b}$$

The weight factor w is the larger the “better” a ray-end with slight precipitation can be detected. A “good” ray end means e.g. that it is:

- at least, say, 5 km long,
- with small reflectivity (say, below 20 dBZ),
- but sufficiently above noise (SNR say > 10 dB),
- with small dBZ and ZDR variability (stddev say < 5dB for dBZ, < 2dB for ZDR),
- not too far away from the last (i.e. outmost) dBZ echoes,
- with total Phi being significant.

The weight factor w is calculated based on that parameters.

7) Attenuation Correction only for Rain

If *Attenuation Correction only below Freezing level* is selected, the attenuation correction is done only for range gates below the freezing level. With this selection, the correction is only applied for rain, where the parameters used in the above equations usually are selected for. In regions above the freezing level, where precipitation can be assumed to be snow, the specific attenuation $\delta A/\delta r$ is set to zero.

The freezing level can be selected in the PDF in km above MSL, or it can be read from a file. The second choice allows – by continuous update of the freezing level information file using external tools – to always use the correct freezing level information for the given time stamp of the radar data.

8) Format of freezing level data file

The freezing level data has to be located in the subdirectory **`sensordata`**. Valid filenames are **`*.freezelevel`**. Such a file consists only of an ASCII part in XML format:

```
<?xml version="1.0"?>
<freezelevel>
   <!-- If this file is used, it must contain at least one <fl> entry -->
   <fl datetime="2004-10-12T00:30:00" height="2.120"/>
   <fl datetime="2004-10-12T06:30:00" height="2.423"/>
   <fl datetime="2004-10-12T12:30:00" height="3.225"/>
   <fl datetime="2004-10-12T18:30:00" height="3.021"/>
   <fl datetime="2004-10-13T00:30:00" height="2.530"/>
   <fl datetime="2004-10-13T06:30:00" height="2.346"/>
   <fl datetime="2004-10-13T12:30:11" height="3.125"/>
</freezelevel>
```

Meaning of the parameters:

Tag/Attr./Cell	Description
`fl`	Freezing level data line
`datetime`	Date & time stamp of freezing level detection
`height`	Height of freezing level in [km]

Always that "fl" entry is used by the algorithm which is closest to the product time stamp. If the product time stamp is in between two "fl" entries of a time series, the freezing level height is calculated as a linear weighted mean of the two neighboring time stamps.

13 References

Anagnostou, M.N., E.N. Anagnostou, G. Vulpiani, M. Montopoli, F.S. Marzano, and J. Vivekanandan (2008): *Evaluation of X-band polarimetric-radar estimates of drop-size distributions from coincident S-band polarimetric estimates and measured raindrop spectra*. IEEE Trans. Geosci. Rem. Sens. **46** (10), pp. 3067-3075.

Andrieu, H., and J.D. Creutin (1995): *Identification of vertical profiles o radar reflectivities for hydrological applications using an inverse method. Part I: Formulation.* J. Appl. Meteor., **34**, pp. 225-239.

Atlas, D. (1954): *The estimation of cloud parameters by radar*. J. Meteorol., **11**, pp. 309-317.

Balakrishnan, N. and D.S. Zrnić (1990): *Use of polarization to characterize precipitation and discriminate large hail.* J. Atmos. Sci., **47**, pp. 1525-1540.

Battan, L.J. (1973): *Radar observations of the atmosphere.* Univ. of Chicago Press, Chicago, 323 p.

Biggerstaff, M.I., and S.A. Listemaa (2000): *An improved scheme for convective/stratiform echo classification using radar reflectivity.* J. Appl. Meteorol., **39**, pp. 2129-2150.

Brandes, E.A., G. Zhang, and J. Vivekanandan (2004): *Comparison of polarimetric radar drop size distribution retrieval algorithms.* J. Atmos. Ocean. Technol. **21** (4), pp. 584-598.

Bringi, V.N., T.D. Keenan and V. Chandrasekar (2001): *Correcting C-band radar reflectivity and differential reflectivity data for rain attenuation: A self-consistent method with constraints.* IEEE Trans. Geosci. Remote Sens., **39**, 1906-1915.

Brown, E.N., and Braham, R.R.Jr. (1963): *Precipitation particle measurements in cumulus congestus*. J. Atmos. Sci., **20**, pp. 23-28.

Campbell, S. D. (1989): *Use of features aloft in the TDWR microburst recognition algorithm*. 24th Conf. on Radar Meteorology, Tallahassee (Fld.), USA, pp.167-170.

Depue, T.K., P.C. Kennedy, and S.A. Rutledge (2007): *Performance of the Hail Differential Reflectivity (HDR) Polarimetric Radar Hail Indicator*. J. Appl. Meteor. Clim., **46**, pp. 1290-1301.

References

Dokter, A.M., F. Liechti and I. Holleman (2009): *Bird detection by operational weather radar*. KNMI Scientific report WR 2009-06.
Available online at http://www.knmi.nl/bibliotheek/knmipubWR/WR2009-06.pdf
(status of September 2010)

Dokter, A.M., F. Liechti, H. Stark, L. Delobbe, P. Tabary and I. Holleman (2010): Bird migration flight altitudes studied by a network of operational weather radars. Journal of the Royal Society Interface, 2010, doi:10.1098/rsif.2010.0116.
Available online at
http://www.knmi.nl/publications/fulltexts/dokter2010rsif_bird_migration.pdf
(status of September 2010).

Dotzek, N., and T. Fehr (2003): *Relationship between precipitation rates at the ground and aloft - a modeling study*. J. Appl. Meteor., **42**, pp. 1285-1301.

Douglas, R.H. (1964): *Hail size distribution*. Proc. 11th Weather Radar Conf., pp. 146-149.

Eilts, M.D., S.H. Olson, G.J. Stumpf, L.G. Hermes, A. Abrevaya, J. Culbert, K.W. Thomas, K. Hondl, and D. Klingle-Wilson (1991): *An improved gust front detection algorithm for the TWDR*. 25th Int. Conf. Radar Meteorol., Paris, J37–J42.

Evenden, G.I. (2003): *Cartographic Projection Procedures for the UNIX Environment - A User's Manual*. U.S. Department of the Interior Geological Survey, Open-File Report 90-284.

Fedorov, A.A., V.D. Stepanenko (1978): *Radar Identification of Dust Storms.* T. Vyp. 411, Glav. Geof. Obs, Leningrad, pp 71-75. (in Russian)

Féral, L., H. Sauvageot, and S. Soula (2003): *Hail Detection Using S- and C-Band Radar Reflectivity Difference.* J. Atmos. Oceanic Technol., **20**, 233-248.

Frehlich, R., L. Cornman (2002): *Estimating Spatial Velocity Statistics with Coherent Doppler Lidar.* J. Atmos. Oceanic Technol., **19**, 355-366.

Gematronik (2007): *Dual-Polarization Weather Radar Handbook, 2nd Edition. V.N. Bringi, M. Thurai, R. Hannesen (Ed.).* Selex-SI Gematronik, 163 pp.

Ghobrial, S.I., S.M. Sharief (1987): *Microwave Attenuation and Cross Polarization in Dust Storms.* IEEE Trans. Antennas Propag. AP-35 (4), pp 418-425.

Goldhirsch, J. (1982): *A Parameter Review and Assessment of Attenuation and Backscatter Properties Associated with Dust Storms over Desert Regions in the Frequency Range of 1 to 10 GHz.* IEEE Trans. Antennas Propag. AP-30 (6), pp 1121-1127.

Gorgucci, E., V. Chandrasekar, and V.N. Bring (2002): *Drop size distribution retrieval from polarimetric radar measurements*. Proc. 2nd Europ. Conf. Radar Meteorol. Hydrol. (ERAD), Delft, Netherlands, pp. 134-139.

Gourley, J.J., P. Tabary and J. Parent du Chatelet (2007): A fuzzy logic algorithm for the separation of precipitation from non-precipitating echoes using polarimetric radar observations, J. Atmos. Oceanic Tech, **24**, pp. 1439-1451.

Hannesen, R., A. Weipert (2003): *Detection of Dust Storms with a C-Band Doppler Radar.* Preprints, 31st Int. Conf. on Radar Meteorology, AMS, Seattle (USA).

Hannesen, R., and H. Gysi (2002): *An enhanced precipitation accumulation algorithm for radar data*. European Conference on Radar Meteorology, ERAD Publication Series Vol. **1**, pp. 266-271.

Hannesen, R., and M. Löffler-Mang (1998): *Improvement of quantitative rain measurements with a C-band Doppler radar through consideration of orographically induced partial beam screening*. Proc. COST 75 Seminar, Switzerland, 23-27 March 1998 (European Commission EUR 18567 EN), pp. 511-519.

Harris, D.M., and W.I. Rose (1983): *Estimating particle sizes, concentrations, and total mass of ash in volcanic clouds using weather radar.* J. Geophys. Res. **88**, pp. 10969-10983.

Hitschfeld, W., and J. Bordan (1954): *Errors inherent in the radar measurement of rainfall at attenuating wavelengths*. J. Meteorol., **11**, pp. 508–514.

Holleman, I. (2001): *Hail detection using single-polarization radar*. KNMI De Bilt (Netherlands), Scientific report WR-2001-01.

Holton, J.R. (1992): *An introduction to dynamic meteorology*. Academic Press, San Diego (CA), 511 pp.

Hubbert, J. and V.N. Bringi (1995): *An iterative filtering technique for the analysis of copolar differential phase and dual-frequency radar measurements.* J. Atmos. Oceanic Technol., **12**, 643-648.

Kammer, A. (1991): *A low-cost X-band radar system designed for the use in urban hydrology*. Proc. 25th Int. Conf. Radar Meteorol., Paris, France, 24-28 June 1991, pp 844–847.

Keenan, T.D. (2003): Hydrometeor classification with a C-band polarimetric radar, Aust. Meteor. Mag., **52**, 23-31.

Maki, M., et al. (2001): *Observations of Volcanic Ashes with a 3-cm Polarimetric Radar.* 30th Conf. on Radar Meteorology, Munich (Germany), pp 226-228.

References

Marecal, V., T. Tani, P. Amayenc, C. Klapisz, E. Obligis, and N.Viltard (1997): *Rain relations inferred from microphysical data in TOGA COARE and their use to test a rain-profiling method from radar measurements at Ku-band.* J. Appl. Meteorol., **36**, 1629–1646.

Marshall, J. S., and Palmer, W. Mc. (1948): *The distribution of raindrops with size*. J. Meteorol., **5**, pp. 165-166.

Marzano F.S., S. Barbieri, G. Vulpiani and W.I. Rose (2006): *Volcanic ash cloud retrieval by ground-based microwave weather radar.* IEEE Trans. Geosci. Rem. Sens., **44**, pp. 3235-3246.

Mitchell, E. D.W., S. V. Vasiloff, G. J. Stumpf, A. Witt, M D. Eilts, J. T. Johnson, K. W. Thomas (1998): *The National Severe Storms Laboratory Tornado Detection Algorithm.* Wea. Forecasting, **13**, pp. 352–366

Nexrad Algorithm Report (1985): *Mesocyclone Detection Algorithm*, NX-DR-002/34.

Ola, P., G. Persson, T. Andersson (1987): *Automatic wind field interpretation of Doppler radar wind components*. SMHI Promis Rapporter Nr 6, December 1987.

Press, W.H., S.A.Teukolsky, W.T. Vetterling, and B.P. Flannery (1992): *Numerical recipes in C. The art of scientific computing.* Cambridge Univ. Press (2nd Edition), New York, 994 p.

Rowe, A., P.L. Heinselman, and T. Schuur (2004): *Estimating hail size using polarimetric radar.* Report, NWS Research Experiences for Undergraduates, 24pp. Available online at http://www.caps.ou.edu/reu/reu04/Angela Rowe Final Paper.pdf (status of March 2009)

Ryzhkov, A. and D.S. Zrnić (1995): *Precipitation and attenuation measurements at 10 cm wavelength.* J. Appl. Meteor., **34**, 2121–2134.

Ryzhkov, A., S.E. Giangrande and T.J. Schuur (2005): Rainfall estimation with a polarimetric prototype of WSR-88D, J Appl. Meteor, **44**, pp 502-515.

Schuur, T., A. Ryzhkov and P. Heinselman (2003): Observations and classification of echoes with the polarimetric WSR-88D radar, NOAA National Severe Storms Laboratory Tech Report, Norman, Oklahoma, USA.

Semenov, O.E. (1997): *Experimental Investigations of the Wind Profiles and Sand Discharge During Sand Storms.* First LAS/WMO Int. Symp. on Sand and Dust Storms, Damascus, WMO/TD-No. 864 (1998), pp 139-150.

Smith, C.J. (1986): *The reduction of errors caused by bright bands in quantitative rainfall measurements made using radar*. J. Atmos. Oceanic Technol., **3**, pp. 129-141.

Steiner, M., Houze Jr, R.A., and Yuter, S (1995): *Climatological characterization of three-dimensional storm structure from operational radar and rain gauge data*. J. Appl. Meteor., **34**, pp. 1978–2007

Testud, J, E. Le Bouar, E. Obligis, and M. Ali-Mehenni (2000): *The rain profiling algorithm applied to polarimetric weather data.* J. Atmos. Oceanic Technol. **17**, 332–356.

van de Hulst, H.C. (1981): *Light scattering by small particles.* Dover Publications, 994 p.

Waldteufel, P. and Corbin, H. (1979): *On the analysis of single Doppler data*. J.Appl. Meteorol. **18**, pp. 532-542.

Waldvogel, A., Federer, B., and P. Grimm (1979): *Criteria for the detection of hail cells*. J.Appl. Meteorol. **18**, pp. 521-525.

Witt, A., Eilts, M.D., Stumpf, G.J., Johnson, J.T., Mitchell, E.D., and Thomas, K.W. (1998): *An Enhanced Hail Detection Algorithm for the WSR-88D*. Wea. Forecast. **13**, pp. 286-303.

WMO (1995): Manual on Codes (International Codes), Volume I.2, WMO-No. 306.

Zgonc, A. and J. Rakovec (1998): *Time extrapolation of radar echo patterns*. Proc. COST 75 seminar, Locarno, Switzerland, 23 to 27 March 1998, 229–238.

Zhang, P., P.W. Chan, R. Doviak, and Fang, M. (2009): *Estimate of Eddy Dissipation Rate Using Spectrum Width Observed by the Hong Kong TDWR Radar*. Proc. 34th Int. Conf. Radar Meteorol., Williamsburg, VA, USA, 5-9 October 2009, P6.9.